Articles

Comparison of the Thermotropic and Solution Behavior of Six-Arm Star and Comb Poly[11-(4′-cyanophenyl-4″-phenoxy)undecyl acrylate]s

Andrea M. Kasko and Coleen Pugh*

Department of Polymer Science, Maurice Morton Institute of Polymer Science, The University of Akron, Akron, Ohio 44325-3909

Received April 10, 2006; Revised Manuscript Received June 29, 2006

ABSTRACT: "Six-arm star" poly[11-(4′-cyanophenyl-4″-phenoxy)undecyl acrylate]s with 13−112 (gel permeation chromatography, GPC, relative to linear polystyrene) or 23−756 (GPC using a light scattering detector) repeat units were synthesized from the hexafunctional initiator, 1,2,3,4,5,6-hexa((4′-methyl(2″-bromopropionate)-phenoxymethyl)benzene, by atom transfer radical polymerization of 11-(4′-cyanophenyl-4″-phenoxy)undecyl acrylate, followed by fractionation to narrow the polydispersity to 1.06−1.57. The absolute molecular weight, size, and shape of these polymers were characterized by light scattering in CH_2Cl_2, and their thermotropic behavior was analyzed by differential scanning calorimetry; both types of properties were compared to those of the other architectures, especially the corresponding comb poly[11-(4′-cyanophenyl-4″-phenoxy)undecyl acrylate]s with six branches. The solution and thermotropic behavior of the six-arm star and comb polymers are similar.

Introduction

In contrast to low molar mass liquid crystals, side-chain liquid crystalline polymers (SCLCPs) prepared by nonliving polymerizations generally exhibit very broad phase transitions.[1] This was immediately dismissed in the SCLCP literature as being due to polydispersity in molecular weight, which was supported by a fractionation study of poly[11-(4′-cyanophenyl-4″-phenoxy)undecyl acrylate] prepared by conventional radical polymerization.[2] However, we have provided evidence that the broad smectic A to isotropic (s_A−i) phase transition of this polymer is due to the limited miscibility of a mixture of branched structures. Not only do the polydispersity combined with the chain transfer constant to polymer ($C_p = 5.48 \times 10^{-3}$)[3] demonstrate that a conventional radical polymerization of 11-(4′-cyanophenyl-4″-phenoxy)undecyl acrylate generates a mixture of linear and variously branched structures, but the breadth of the isotropization biphasic region of 1:1 binary blends of individual molecular architectures of poly[11-(4′-cyanophenyl-4″-phenoxy)-undecyl acrylate]s increases relatively linearly with the difference in end group densities of the two components, regardless of the combination of topologies or the type of end groups. [4,5]

Thus far, we have investigated linear,[5,6] three-arm star,[6] and comb[4] architectures, which we synthesized by atom transfer radical polymerization (ATRP[7]). The isotropization transitions of all of the poly[11-(4′-cyanophenyl-4″-phenoxy)undecyl acrylate]s produced by ATRP, including those with broad polydispersities, are narrow, suggesting that they have rather uniform topologies. The transition temperatures of these polymers also decrease with increasing branching at identical molecular weights (determined by gel permeation chromatography relative to linear polystyrene, GPC_{PSt}), although they extrapolate to essentially the same values (g 17 s_C 27 s_A 146 i)[8] at infinite molecular weight due to the insignificance of the limited number of end groups and branch points at high molecular weight.

Therefore, the differences in the thermotropic behavior of the polymers are consistent with their designed architectures. However, better support for the different topologies was provided by their solution properties. We investigated the solution behavior of the "linear", "three-arm star", and "comb" poly-[11-(4′-cyanophenyl-4″-phenoxy)undecyl acrylate]s by GPC_{PSt} and light scattering measurements in order to correlate their size and shape with their molecular architectures, and in order to investigate the extent of branching in the corresponding polymer produced by conventional radical polymerization.[9] The solution behavior of the polymer prepared by conventional radical polymerization demonstrated that it was more branched than the linear polymers prepared by ATRP, and the solution properties of the polymers produced by ATRP were consistent with the extent of branching increasing from "linear" to "three-arm star" to "comb" topologies according to their synthetic design. For example, the error in the GPC_{PSt}-determined molecular weights increased, the tendency to aggregate in solution decreased, and the root-mean-square radius of gyration ($\langle R_g^2 \rangle^{1/2}$) in CH_2Cl_2 decreased with increasing branching. The value of the contraction factor, $g = \langle R_g^2 \rangle_{br} / \langle R_g^2 \rangle_{lin}$, of the "comb" polymer was also lower than that of the "three-arm star" polymer in CH_2Cl_2.

This paper further investigates the effect of molecular architecture on the thermotropic and solution properties of SCLCPs by providing a more subtle variation in topology. We have synthesized the six-arm star poly[11-(4′-cyanophenyl-4″-phenoxy)undecyl acrylate]s shown in Scheme 1 as architectural analogues of the comb polymers. The comb polymers were

* To whom correspondence should be addressed.

10.1021/ma060807x CCC: $33.50
Published on Web 09/02/2006

Scheme 1. Comparison of the Molecular Structure and Architecture of Comb[4] and Six-Arm Star Poly[11-(4′-cyanophenyl-4″-phenoxy)undecyl acrylate]s

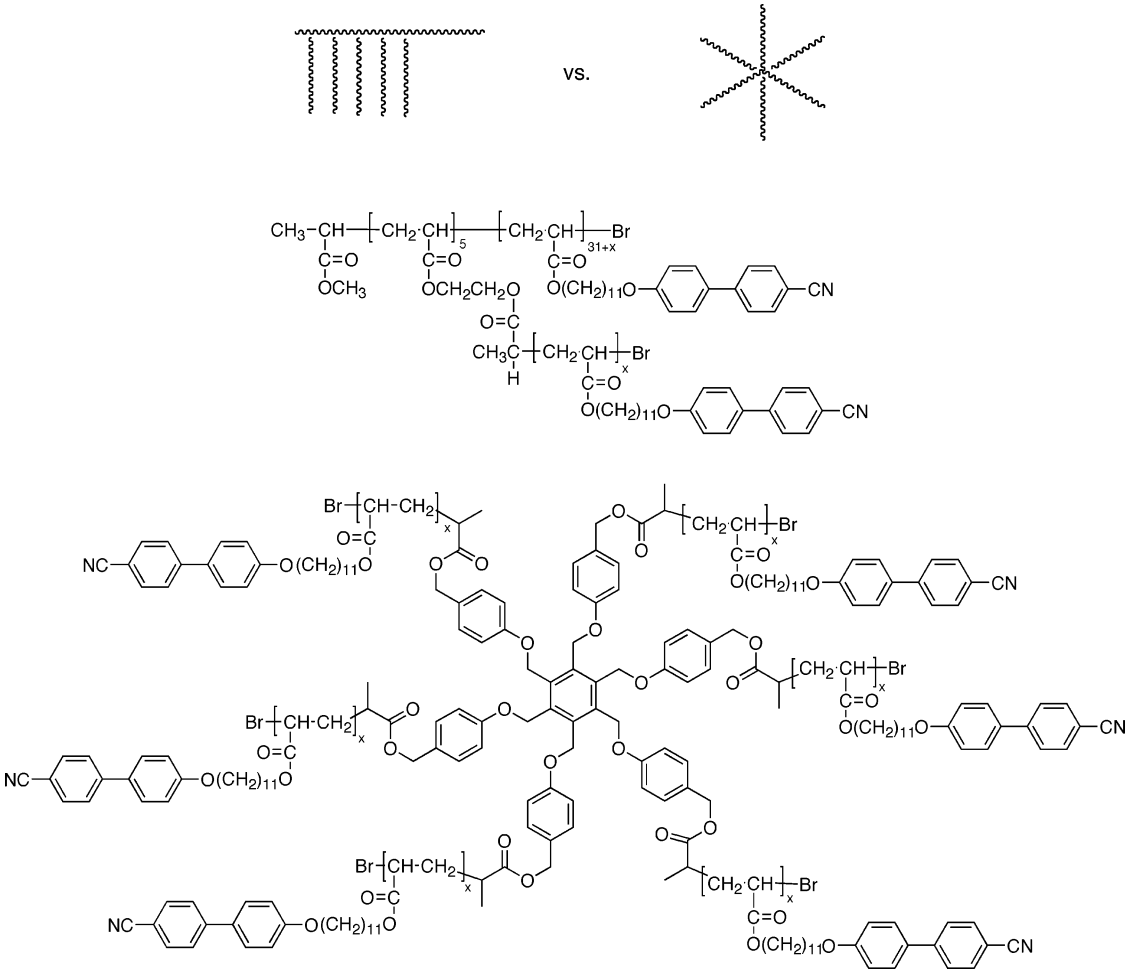

synthesized using a multifunctional macroinitiator.[4] According to combined ^{1}H NMR and absolute molecular weight analyses, the comb polymers contain five SCLCP branches along the polymer backbone separated by an average of five mesogenic repeat units, with a sixth branch resulting from growth at the chain end of the macroinitiator upon grafting; the six branches vary in length from an average of 4−34 repeat units.[10] Therefore, both the six-arm star and comb polymers presumably contain six SCLCP branches, but with different arrangements of those branches. This paper therefore compares the solution and thermotropic properties of the "six-arm star" and comb polymers. We also present the thermotropic behavior of binary blends of the six-arm star polymers with all of the topologies of the corresponding polymers synthesized thus far.

Experimental Section

Materials. 2-Bromopropionyl chloride (Acros, tech.), cuprous bromide (CuBr, Aldrich, 99.999%), 1,2,3,4,5,6-hexamethylbenzene (Aldrich, 98%), 4-hydroxymethylphenol (Avocado Chemicals, 98%), sodium hydride (NaH, Acros, 95%), and trifluoroacetic acid (Aldrich, 99%) were used as received. 2,2′-Azobis(isobutyronitrile) (AIBN, Pfaltz and Bauer, 98%) was recrystallized from methanol below 40 °C, and then stored at −20 °C. *N*-Bromosuccinimide (NBS, Arapahoe Chemicals) was recrystallized from boiling water after hot filtration. Triethylamine (NEt_3, Fisher) was distilled from KOH under N_2 and stored over KOH. 11-(4′-Cyanophenyl-4″-phenoxy)undecyl acrylate[6] and 4,4′-diheptyl-2,2′-bipyridine[6] were prepared as described previously. The linear poly[11-(4′-cyanophenyl-4"-phenoxy)undecyl acrylate]s,[4,5] three-arm star polymers initiated from tris(bromomethyl)mesitylene[6] and 1,3,5-tri(methyl 2-bromopropionate)benzene,[11] and the comb poly[11-(4′-cyanophenyl-4″-phenoxy)undecyl acrylate]s[4] used in blends were synthesized previously by ATRP. Benzene was washed with H_2SO_4, stored over $CaCl_2$, distilled from CaH_2 under N_2, and then stored over type 4 Å molecular sieves. Dimethylformamide (DMF) was distilled in vacuo from type 4 Å molecular sieves under N_2 and stored over type 4 Å molecular sieves. Reagent grade tetrahydrofuran (THF) was dried by distillation from purple sodium benzophenone ketyl under N_2. All other solvents were commercially available and used as received. THF was distilled from $LiAlH_4$ for light scattering measurements. All other HPLC grade solvents were commercially available and used as received.

Techniques. All reactions were performed under a N_2 atmosphere using a Schlenk line unless noted otherwise. Elemental analyses were performed on a Perkin-Elmer 2400 Series II CHNS/O analyzer. ^{1}H NMR spectra (δ, ppm) were recorded on either a Varian Gemini 300 (300 MHz) or a Varian Gemini 200 (200 MHz) spectrometer. All spectra were recorded in $CDCl_3$ or DMSO-d_6, and the resonances were measured relative to residual solvent and referenced to tetramethylsilane. Number- (M_n) and weight-average (M_w) molecular weights relative to linear polystyrene and polydisperisties (PDI = M_w/M_n) were determined by gel permeation chromatography (GPC_{PSt}) at 35 °C using THF ($GPC_{PSt,THF}$) or CH_2Cl_2 (GPC_{PSt,CH_2Cl_2}) as solvent (1.0 mL/min), a set of 50, 100, 500 , and 10^4 Å and linear (50−10^4 Å) Styragel 5 μm columns, a Waters 486 tunable UV/vis detector set at 275 nm, a Waters 410 differential refractometer, and Millenium Empower 2 software. Absolute molecular weights were determined by GPC with a light scattering detector (GPC_{LS}) at 35 °C using CH_2Cl_2 as solvent (1.0 mL/min), a set of 50, 500, and 10^4 Å and linear (50−10^6 Å) Phenogel 5 μm columns, and a Wyatt Technology miniDAWN three-angle (46,

90, and 134°) light scattering detector equipped with a Ga−As laser (690 nm, 20 mW), with the concentration at each elution volume determined using a Wyatt Optilab 903 interferometeric differential refractometer (690 nm). The molecular weight data were calculated using Astra 4.90.07 software (Wyatt Technology) and a Zimm fit. The refractive index (RI) increments ($dn/dc = 0.176$ mL/g in CH_2Cl_2) measured previously[9] at room temperature at 690 nm were used to determine the mass concentrations at each elution volume and the physical constant K^* for the light scattering measurements. The root-mean-square radii of gyration in CH_2Cl_2 were measured from GPC chromatograms under the same conditions, except that a Wyatt Technology DAWN-EOS 18-angle (20−153°) light scattering detector equipped with a Ga−As laser (690 nm, 30 mW) was used instead of the miniDAWN detector. All samples (approximately 0.5 g/L) were dissolved overnight and filtered through a 0.45 μm PTFE filter.

A Perkin-Elmer Pyris 1 differential scanning calorimeter was used to determine the thermal transitions, which were read as the maximum or minimum of the endothermic or exothermic peaks, respectively. Glass transition temperatures (T_gs) were read as the middle of the change in heat capacity. All heating and cooling rates were 10 °C/min. Transition temperatures were calibrated using indium and benzophenone standards, and enthalpy changes were calibrated using indium. All polymers and their blends were dried overnight in vacuo at room temperature before analyzing their thermotropic behavior. The DSC traces of the binary unmixed samples were generated by computer summing the two traces of the individual components.

Synthesis of 1,2,3,4,5,6-Hexa(bromomethyl)benzene. 1,2,3,4,5,6-Hexa(bromomethyl)benzene was synthesized in 12−92% yield as in the following example. 1,2,3,4,5,6-Hexamethylbenzene (3.2 g, 20 mmol), *N*-bromosuccinimide (32 g, 0.18 mol), and AIBN (0.60 g, 3.6 mmol) were stirred at reflux in benzene (100 mL) for 24 h. The reaction mixture was cooled to room temperature and excess bromine was quenched with sodium metabisulfite. The precipitate was collected in a fritted glass filter and washed successively with acetone, CH_2Cl_2 and methanol, and dried in vacuo to obtain a white powder. The crude product was purified by subliming off all impurities at ~225 °C/1 mmHg for 3 days to yield 12 g (92%) of 1,2,3,4,5,6-hexa(bromomethyl)benzene as a white crystalline solid. ^{1}H NMR (DMSO-d_6): 4.86 (s, CH_2Br, 12 H). Anal. Calcd: C, 22.68; H, 1.90. Found: C, 22.79; H, 1.81.

Synthesis of 1,2,3,4,5,6-Hexa[(4′-hydroxymethyl)phenoxymethyl]benzene. A solution of sodium hydride (0.24 g, 95 mmol) in DMF (2 mL) was added dropwise to a solution of 4-hydroxymethylphenol (1.3 g, 0.10 mol) in DMF (2 mL) at room temperature. The solution was then heated to 90 °C, and it turned to a deep blue-green color. After 35 min, 1,2,3,4,5,6-hexa(bromomethyl)benzene (1.0 g, 16 mmol) was added, and the reaction was stirred at 90 °C for 21 h. Excess DMF was distilled off in vacuo, and the crude solid product was passed through a short column of basic alumina using EtOH/toluene (1:1) as the eluant to remove any unreacted phenol. The solvent was removed by rotary evaporation to yield a viscous liquid, and acetone was added to the viscous liquid residue. The resulting solid precipitate was collected in a fritted glass filter and dried in vacuo to yield 1.2 g (86%) of 1,2,3,4,5,6-hexa[(4′-hydroxymethyl)phenoxymethyl]benzene as a white solid. ^{1}H NMR (DMSO-d_6): 4.34 (d, CH_2OH, 12 H), 4.97 (t, OH, 6 H), 5.16 (s, CH_2OAr, 12 H), 6.89 (d, 12 aromatic H ortho to OCH_2), 7.14 (d, 12 aromatic H ortho to CH_2O).

Synthesis of 1,2,3,4,5,6-Hexa[4′-methyl-(2″-bromopropionate)-phenoxymethyl] benzene. A solution of 2-bromopropionyl chloride (2.9 g, 17 mmol) in THF (5 mL) was added dropwise over 20 min to a solution of 1,2,3,4,5,6-hexa[(4′-hydroxymethyl)phenoxymethyl]-benzene (1.5 g, 1.7 mmol) and NEt_3 (2.0 g, 20 mmol) in THF (50 mL) at room temperature. After being stirred at room temperature for 16 h, the reaction mixture was poured into ice water (200 mL). The aq layer was extracted five times with CH_2Cl_2 (50 mL each). The combined organic layers were washed sequentially with dilute aqueous HCl (50 mL), saturated aqueous $NaHCO_3$ (50 mL), and water (30 mL), and then dried over Na_2SO_4. After filtration, the solution was concentrated and purified by flash chromatography using silica gel (5 in.) topped with basic activated alumina (1 in.) as the stationary phase and CH_2Cl_2 as the eluant ($R_f = 0.43$). The solvent was removed via rotary evaporation to yield a yellow oil, which was crystallized from a mixture of ethanol (100 mL) and toluene (20 mL), and recrystallized from ethanol (250 mL) to yield 1.3 g (44%) of 1,2,3,4,5,6-hexa[4′-methyl-(2"-bromopropionate)-phenoxymethyl]benzene as a white powder. ^{1}H NMR ($CDCl_3$): 1.80 (d, CH_3, 18 H), 4.38 (q, CH, 6 H), 5.15 (s, CH_2O_2C, 12 H), 5.18 (s, CH_2OAr, 12 H), 6.87 (d, 12 aromatic H ortho to OCH_2), 7.26 (d, 12 aromatic H ortho to CH_2). Anal. Calcd: C, 50.73; H, 4.26. Found: C, 50.83; H, 4.38.

Scheme 2. Synthesis of 1,2,3,4,5,6-Hexa[4′-methyl(2″-bromopropionate)phenoxymethyl]-benzene, Where NBS = *N*-bromosuccinimide, AIBN = 2,2′-Azobis(isobutyronitrile), DMF = Dimethylformamide, and THF = Tetrahydrofuran

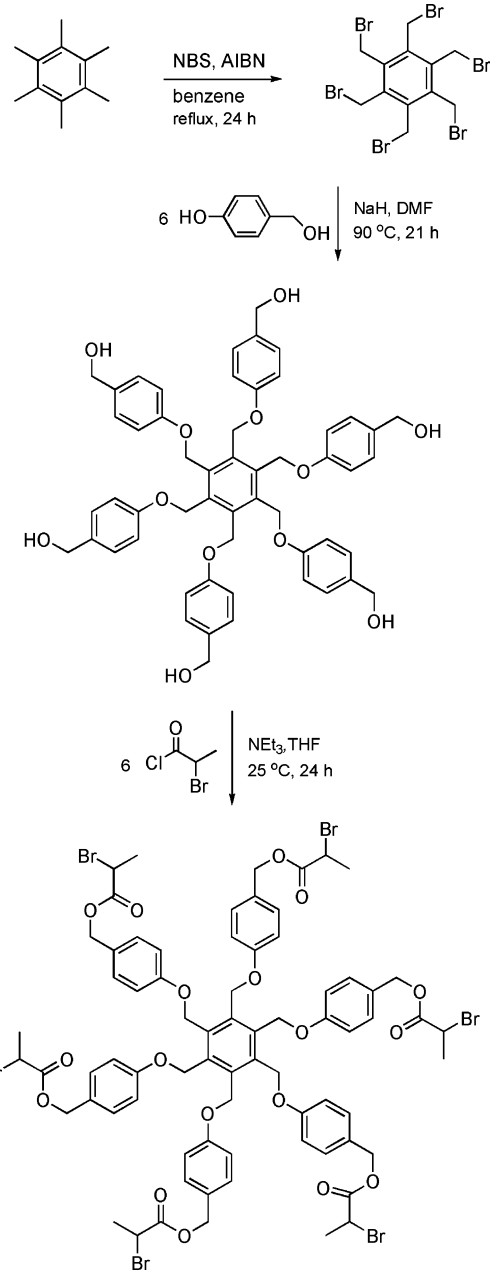

Atom Transfer Radical Polymerization of 11-(4′-Cyanophenyl-4″-phenoxy)undecyl Acrylate Using 1,2,3,4,5,6-Hexa[4′-methyl-(2″-bromopropionate)phenoxymethyl]benzene as the Initiator. The catalyst (60 mM) and ligand (0.18 M) were measured from a benzene solution, prepared by adding benzene to CuBr (43 mg, 0.30 mmol) and 4,4′-diheptyl-2,2′-bipyridine (0.32 g, 0.90 mmol)

Scheme 3. Synthesis of Six-Arm Star Poly[11-(4′-cyanophenyl-4″-phenoxy)undecyl acrylate]s (Scheme 1) by Atom Transfer Radical Polymerization Using 1,2,3,4,5,6-Hexa[4′-methyl(2″-bromopropionate)phenoxymethyl]benzene as the Initiator, Where dHbipy = 4,4′-Diheptyl-2,2′-dipyridyl

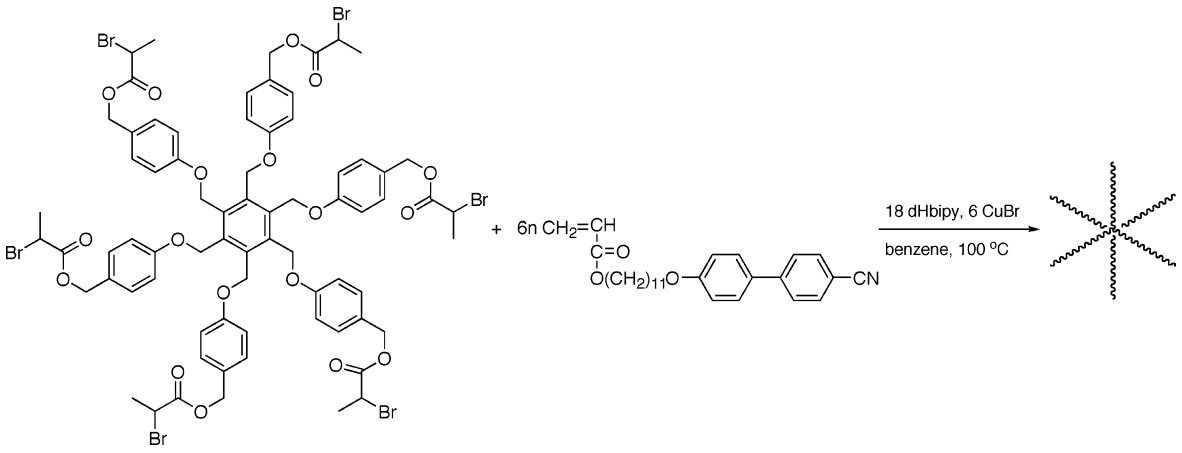

in a 5 mL volumetric flask to a total volume of 5 mL. The initiator was measured from a 12.5 mM solution in benzene, prepared by adding benzene to 1,2,3,4,5,6-hexa[4′-methyl-(2″-bromopropionate)-phenoxymethyl]benzene (85 mg, 0.050 mmol) in a 4 mL volumetric flask to a total volume of 4 mL. In a typical example, a solution of 11-(4′-cyanophenyl-4″-phenoxy)undecyl acrylate (0.50 g, 1.2 mmol), the initiator solution (1.6 mL, 20 μmol) and the catalyst solution (2.0 mL, 0.12 mmol CuBr, 0.36 mmol 4,4′-diheptyl-2,2′-dipyridyl) was degassed by six freeze−pump−thaw cycles in a sealable polymerization tube. The tube was then sealed and the contents were stirred at 100 °C for 16 h. After opening the polymerization tube to air to quench the polymerization, the reaction mixture was diluted with THF (3 mL) and precipitated into a cold (−78 °C) solution of methanol (50 mL) and saturated aqueous NH_4Cl (5 mL). The residue was reprecipitated four times from THF (3 mL) into a cold (−78 °C) solution of methanol (50 mL) and saturated aqueous NH_4Cl (5 mL) to remove copper and excess monomer. After drying in vacuo, the resulting polymer (0.29 g, 57% yield; $GPC_{PSt,THF}$ $M_n = 1.61 \times 10^4$, PDI = 1.14) was dissolved in THF (4 mL), and methanol was added dropwise until the solution became turbid (14 mL methanol). After 2 d, the sample had separated into two phases. The lower THF-rich layer was collected and precipitated into cold (−78 °C) methanol (25 mL) containing 1 drop of conc HCl to yield 0.21 g (42%) of "six-arm star" poly[11-(4′-cyanophenyl-4″-phenoxy)undecyl acrylate as a white solid; $GPC_{PSt,THF}$ $M_n = 1.01 \times 10^4$, PDI = M_w/M_n, = 1.08; GPC_{LS} $M_n = 2.40 \times 10^4$, PDI = 1.12.

Preparation of Blends of Poly[11-(4′-cyanophenyl-4"-phenoxy)undecyl acrylate]s. Binary blends were prepared in quantitative yield by dissolving both components in a minimum amount of THF, precipitating with cold methanol, and removing the solvent and drying the precipitate in vacuo at 60 °C overnight. For example, six-arm star polymer (11.4 mg, $DP_n = 112$, PDI = 1.56) and six-arm star polymer (11.3 mg, $DP_n = 36$, PDI = 1.14) were dissolved in THF (∼0.5 mL), and cold (−78 °C) methanol (∼2 mL) was added dropwise to precipitate the polymer. The sample was dried in vacuo at 60 °C overnight and analyzed directly by $GPC_{PSt,THF}$: $M_n = 4.98 \times 10^4$, PDI = 2.20.

Results and Discussion

Synthesis of Six-Arm Star Polymers by ATRP. As shown in Scheme 2, 1,2,3,4,5,6-hexa[4′-methyl(2"-bromopropionate)-phenoxymethyl]benzene was synthesized by first brominating the benzylic positions of 1,2,3,4,5,6-hexamethylbenzene using *N*-bromosuccinimide and AIBN. The partially brominated side products were removed by sublimation, leaving elementally pure hexa(bromomethyl)benzene as the residue. 1,2,3,4,5,6-Hexa-(bromomethyl)benzene was then etherified with sodium 4′-hydroxymethylphenoxide, and the resulting 1,2,3,4,5,6-hexa((4′-hydroxymethyl)phenoxymethyl)benzene was esterified with 2-bromopropionyl chloride. The resulting initiator was elementally pure.

The hexafunctional initiator shown in Scheme 2 was designed to have minimum steric constraints between initiating sites; i.e., rather than using benzene directly substituted at all six positions with 2-bromopropionate initiating sites, the six initiating sites were attached to the benzene core through a second aromatic ring, such that the closest substituent to each initiating site is at the para position. However, since the chain transfer constant to poly[11-(4′-cyanophenyl-4″-phenoxy)undecyl acrylate] is 5.48×10^{-3},[3] the effect of chain transfer to polymer will only be undetectable if the number-average degree of polymerization (DP_n) is limited to 18 or lower ($DP_n \leq (1/10)C_X$)[12] at high monomer conversion. We therefore used higher monomer-to-initiator ratios for the polymerizations and restricted the monomer conversions to incomplete values to obtain higher molecular weight polymers; this should also minimize star−star coupling.

Scheme 3 presents the atom transfer radical polymerization of 11-(4′-cyanophenyl-4″-phenoxy)undecyl acrylate using the hexafunctional initiator, and Table 1 summarizes the polymerization results. The polydispersities of the resulting polymers were broader than desired, and we therefore fractionated the original polymers to obtain samples with narrower molecular weight distributions. According to the GPC_{PSt} measurements in THF, the chain lengths of the fractionated polymers range from 13 to 112 repeat units (2−19 repeat units per arm), with polydispersities of 1.08−1.56. Table 1 also lists the molecular weight data of the fractionated polymers determined by GPC_{PSt} in CH_2Cl_2, which is a better solvent than THF for these polymers based on little or no aggregation in CH_2Cl_2.[9] According to $GPC_{PSt,CH2Cl2}$, the chain lengths of the fractionated polymers range from four to 94 repeat units (1−16 repeat units per arm), with polydispersities of 1.11−1.75. Although the relative values of the GPC_{PSt} molecular weights determined in CH_2Cl_2 and THF are erratic, the absolute molecular weights determined by GPC_{LS} in CH_2Cl_2 using a three-angle light scattering detector (Table 1) are consistently higher than those determined by either $GPC_{PSt,THF}$ or $GPC_{PSt,CH2Cl2}$. According to GPC_{LS}, the chain lengths of the fractionated six-arm star polymers range from 23 to 756 repeat units (4−126 repeat units per arm), with polydispersities of 1.06−1.57.

Figure 1 plots the absolute number-average molecular weights[13] measured by GPC_{LS} in CH_2Cl_2 as a function of the GPC_{PSt}-determined molecular weights measured in both CH_2Cl_2 and

Table 1. Synthesis of Six-Arm Star Poly[11-(4′-cyanophenyl-4″-phenoxy)undecyl acrylate]s by Atom Transfer Radical Polymerization at 100 °C in Benzene Using 1,2,3,4,5,6-Hexa[4′-methyl-(2″-bromopropionate)phenoxymethyl]benzene as the Initiator[a]

		original polymers				fractionated polymers									
			GPC_{PSt} in THF [c]			yield[e]	GPC_{PSt} in THF [c]			GPC_{PSt} in CH_2Cl_2[c]			GPC_{LS} in CH_2Cl_2[f]		
$[M]_0/[I]_0$	time (h)	yield[b] (%)	$M_n \times 10^{-3}$	DP_n[d]	PDI	(%)	$M_n \times 10^{-3}$	DP_n[d]	PDI	$M_n \times 10^{-3}$	DP_n[d]	PDI	$M_n \times 10^{-3}$	DP_n[d]	PDI
30	56	48	17.3	37	1.48	44	16.7	36	1.14	27.0	60	1.35	56.4	130	1.14
60	24	34	4.12	6	1.33	26	7.36	13	1.14	3.23	4	1.11	11.5	23	1.06
75	56	62	9.26	18	1.28	47	9.56	19	1.16	7.52	14	1.17	12.8	26	1.10
90	56	73	21.6	47	2.00	56	27.0	60	1.30	15.1	32	1.34	61.1	142	1.57
105	56	57	16.1	34	1.14	42	10.1	20	1.08	12.9	48	1.16	24.0	53	1.12
120	48	68	23.9	53	2.33	41	30.2	68	1.45	41.1	94	1.36	150	353	1.27
120	36	37	36.5	83	2.09	16	48.7	112	1.56	24.8	55	1.75	319	756	1.39

[a] Using 6:18:1 [CuBr]:[4,4′-diheptyl-2,2′-dipyridyl]:[Initiator]. [b] After copper and monomer were completely removed by multiple reprecipitations. [c] Number-average molecular weight (M_n), number-average degree of polymerization (DP_n) and polydispersity (PDI = M_w/M_n; M_w = weight-average molecular weight) determined by gel permeation chromatography (GPC_{PSt}) in tetrahydrofuran (THF) or CH_2Cl_2 at 35 °C relative to linear polystyrene using mean of UV and/or RI detectors. [d] $DP_n = (M_n - 1704.79)/419.56$. [e] Total polymerization yield after both purification to remove monomer and initiator, and fractionation. [f] Determined at 35 °C using a three-angle (46, 90, and 134°) light scattering detector.

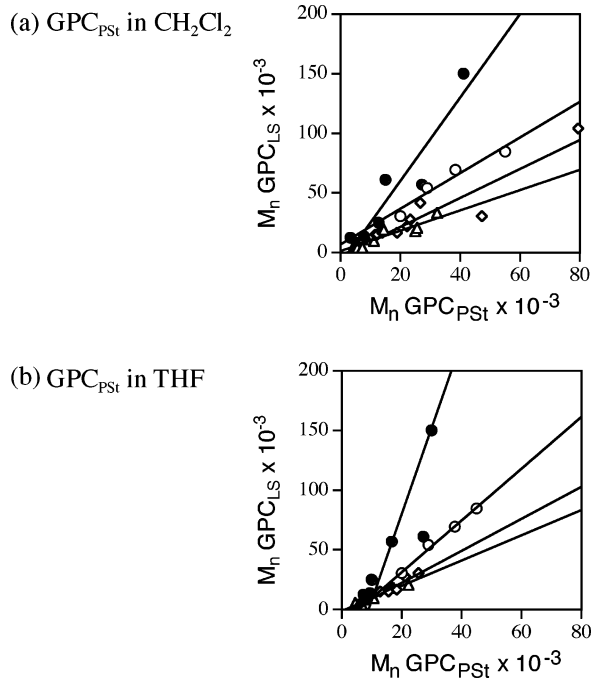

Figure 1. Plots of the number-average molecular weights (M_n) of the six-arm star poly[11-(4′-cyanophenyl-4″-phenoxy)undecyl acrylate]s (●) determined by gel permeation chromatography (GPC) with a light scattering detector (GPC_{LS}) in CH_2Cl_2 as a function of the molecular weights measured by GPC in (a) CH_2Cl_2 and (b) tetrahydrofuran (THF) relative to linear polystyrene (GPC_{PSt}), and in comparison to those plots for the comb (○), three-arm star (◇), and all of the linear (△) polymers reported previously.[9]

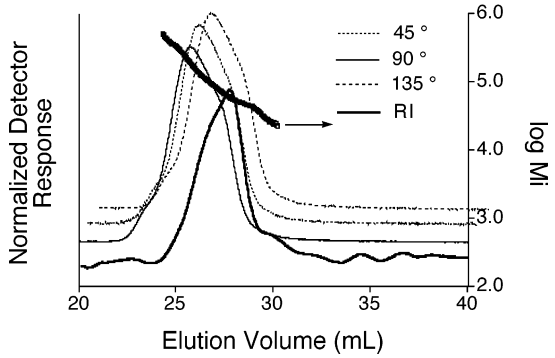

Figure 2. Gel permeation chromatography refractive index (RI) and three of the 18 light scattering detector responses and log M_i calibration curves (□) of the blends of the six-arm star (M_n = 69 300; PDI = 1.61) poly[11-(4′-cyanophenyl-4″-phenoxy)undecyl acrylate]s in CH_2Cl_2.

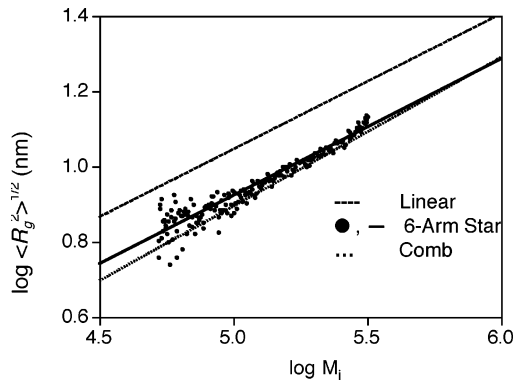

Figure 3. Log−log plot of the root-mean-square radii of gyration ($\langle R_g^2 \rangle^{1/2}$) of the six-arm star (●, $y = 0.36x - 0.90$, least-squares fit) poly[11-(4′-cyanophenyl-4″-phenoxy)undecyl acrylate]s as a function of molecular weight (M_i) in CH_2Cl_2 using the GPC_{LS} chromatograms shown in Figure 2, and comparison to the corresponding least-squares fits of the previously reported[9] comb ($y = 0.39x - 1.1$) and linear polymers ($y = 0.36x - 1.3$).

THF for the six-arm star polymers and, for comparison, the comb, three-arm star, and linear polymers reported previously.[9] The errors in the GPC_{PSt}-determined molecular weights of the six-arm star and comb polymers are higher than those of the three-arm star polymers, which are higher than those of the linear polymers. However, the error in the GPC_{PSt}-determined molecular weights is much higher for the six-arm star polymers than for the comb polymers. This indicates that the six-arm star polymers have the smallest hydrodynamic volumes of all of the architectures at a given molecular weight in CH_2Cl_2, and/or that they interact with the GPC columns more than the other architectures.

Solution Behavior of the Six-Arm Star Polymers. The solution behavior of a polymer can be studied over a broad molecular weight range using a single GPC chromatogram from a sample with a broad molecular weight distribution,[9,14] since each elution slice of the GPC chromatogram corresponds to a single size polymer ($M_n = M_w$) or a fraction of very narrow polydispersity.[15] We therefore blended four of the six-arm star polymers to obtain a sample with DP_n = 161 and PDI = 1.61 according to GPC_{LS} (Table S2 in the Supporting Information), and studied its solution behavior using a light scattering detector with 18 angles. The measured M_n value of the blend is close to that calculated using the composition and M_n values of each component. Figure 2 shows the GPC chromatograms of this six-arm star polymer blend in CH_2Cl_2 monitored by the differential refractometer (RI) detector and the light scattering

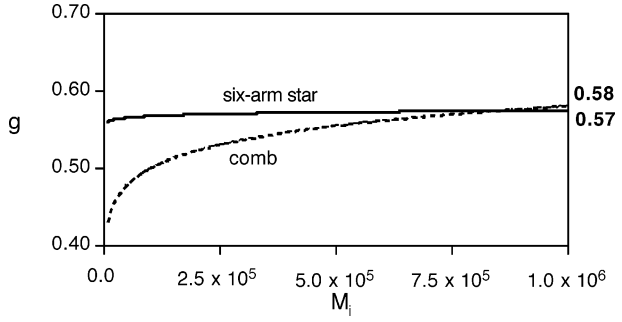

Figure 4. Comparison of the contraction factors ($g = \langle R_g^2\rangle_{br}/\langle R_g^2\rangle_{lin}$ at same molecular weight) of the six-arm star and previously reported[9] comb poly[11-(4′-cyanophenyl-4″-phenoxy)undecyl acrylate]s as a function of molecular weight in CH_2Cl_2 using the lines in Figure 3.

Table 2. Thermotropic Behavior of Six-Arm Star Poly[11-(4′-cyanophenyl-4″-phenoxy)undecyl acrylate]s Synthesized by Atom Transfer Radical Polymerization

GPC_{PSt}[a]		GPC_{LS}[b]		transition temp[c](°C)			
DP_n	PDI	DP_n	PDI	g−s_C	s_C−s_A	s_A−i	peak width[d] fwhm (°C)
13	1.14	23	1.06	6	14	84	8.63
19	1.16	26	1.10	8	14	94	6.27
20	1.08	53	1.12	13	22	112	9.02
36	1.14	130	1.14	14	25	133	5.20
60	1.30	142	1.57	14	25	136	4.52
68	1.45	353	1.27	17	25	138	3.27
112	1.56	756	1.39	15	26	136	4.31

[a] Number-average degree of polymerization ($DP_n = (M_n - 1704.8)/419.56$, M_n = number-average molecular weight) and polydispersity (PDI = M_w/M_n; M_w = weight-average molecular weight) determined by gel permeation chromatography (GPC_{PSt}) in tetrahydrofuran at 35 °C relative to linear polystyrene using mean of UV and/or RI detectors. [b] Determined at 35 °C in CH_2Cl_2 using a three-angle (46, 90, and 134°) light scattering detector. [c] Determined by differential scanning calorimetry on heating at 10 °C/min; g = glass, s_C = smectic C, s_A = smectic A, i = isotropic. [d] Peak width of isotropization determined from the full width at half-maximum of the peak intensity (fwhm).

detector at three of its 18 angles; the chromatograms are corrected for the interdetector delay. The sample is polydisperse, which causes the light scattering chromatograms to shift to lower elution volumes relative to the RI chromatogram.[15] In addition, the shapes of the RI and light scattering chromatograms are slightly different, with the light scattering chromatograms weighted more toward the high molecular weight side, since the light scattering detector response is sensitive to both concentration and molar mass ($\propto c_i M_i$), whereas the RI detector response is only sensitive to concentration (αc_i). Nevertheless, there is no evidence in the light scattering chromatograms of aggregates eluting separately from the main peak at low elution volume, in contrast to the corresponding linear polymers.[9] The slight difference in the shape of the RI and light scattering chromatograms and the lack of aggregation in CH_2Cl_2 are very similar to the chromatography behavior of the comb polymers with six branches.

Figure 2 also includes the calibration curves relating the logarithmic molecular weight to elution volume, with the molecular weight values calculated by extrapolation of the eighteen light scattering responses to zero angle. The calibration curve is fairly linear. Figure 3 plots the root-mean-square radii of gyration calculated from the angular dependence of the scattered light from the chromatogram in Figure 2 at approximately every 8 μL over the molecular weight range 40k−320k; both the molecular weight and $\langle R_g^2\rangle^{1/2}$ calculations assume that the concentration at each elution slice is negligible. The data are most scattered in the lower molecular weight region

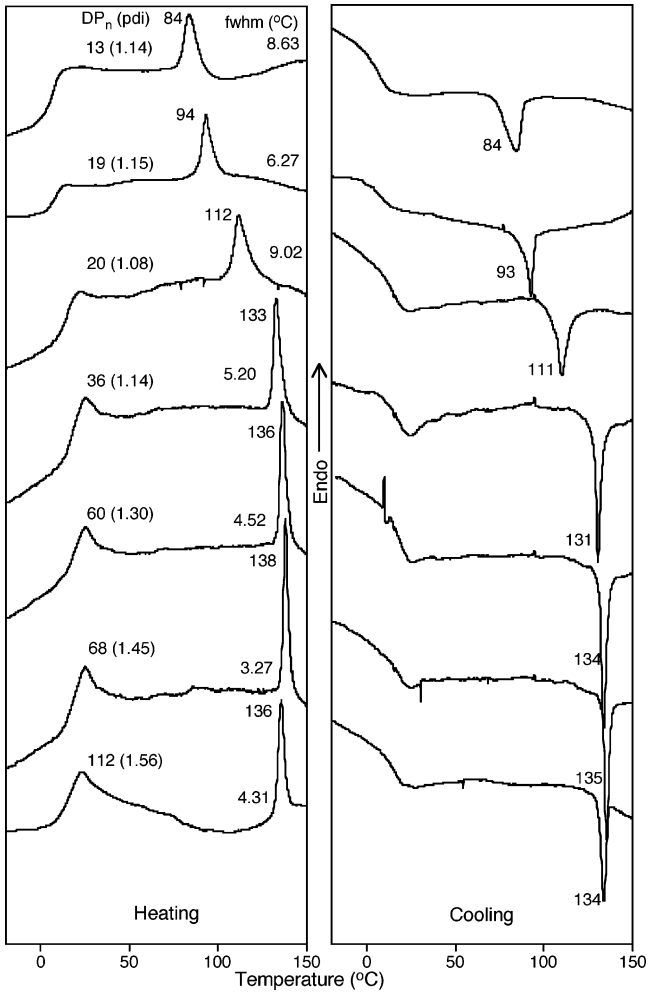

Figure 5. Normalized differential scanning calorimetry traces (10 °C/min) of six-arm star poly[11-(4′-cyanophenyl-4″-phenoxy)undecyl acrylate]s ($GPC_{PSt,THF}$-determined DP_n = 13−112, PDI = 1.08−1.56); fwhm = full width at half-maximum peak intensity.

where the angular dependence is low, and they are close to the limiting molecular weights for calculating $\langle R_g^2\rangle^{1/2}$. For comparison, Figure 3 also includes the least-squares fits of the data reported previously[9] for the corresponding linear and comb polymers. The size of the six-arm star and comb polymers are nearly identical, and both are much more compact than the linear polymers at identical molecular weight.

The slopes of the log−log plots correspond to the scaling coefficients, ν, relating R_g to molecular weight ($R_g = KM^{\nu}$), and are essentially the same for the three architectures (six-arm star, $\nu = 0.36$; comb, $\nu = 0.39$; linear, $\nu = 0.36$), as expected for linear and branched polymers based on the same chemical repeat unit with sufficiently long arms.[16,17] However, these values are smaller than the lower limit of 0.50 for a random coil in a Θ solvent (Gaussian limit),[18] and are approaching the hard sphere limit of 0.33. As we discussed previously,[9] this shows that the average segment density is greater than that for a Gaussian chain and approaches that for a bulk polymer, presumably due to both the long mesogenic side chains in every repeat unit and the strong intramolecular mesogen-mesogen interactions. Therefore, the long mesogenic side chains seem to cause these SCLCPs to behave as more branched structures than the nominal star and comb structures drawn schematically in Scheme 1.

Figure 4 plots the ratio of the least-squares lines in Figure 3 of the six-arm star and linear polymers, i.e., $g = \langle R_g^2\rangle_{br}/\langle R_g^2\rangle_{lin}$, and compares it to the contraction factor (g) of the comb

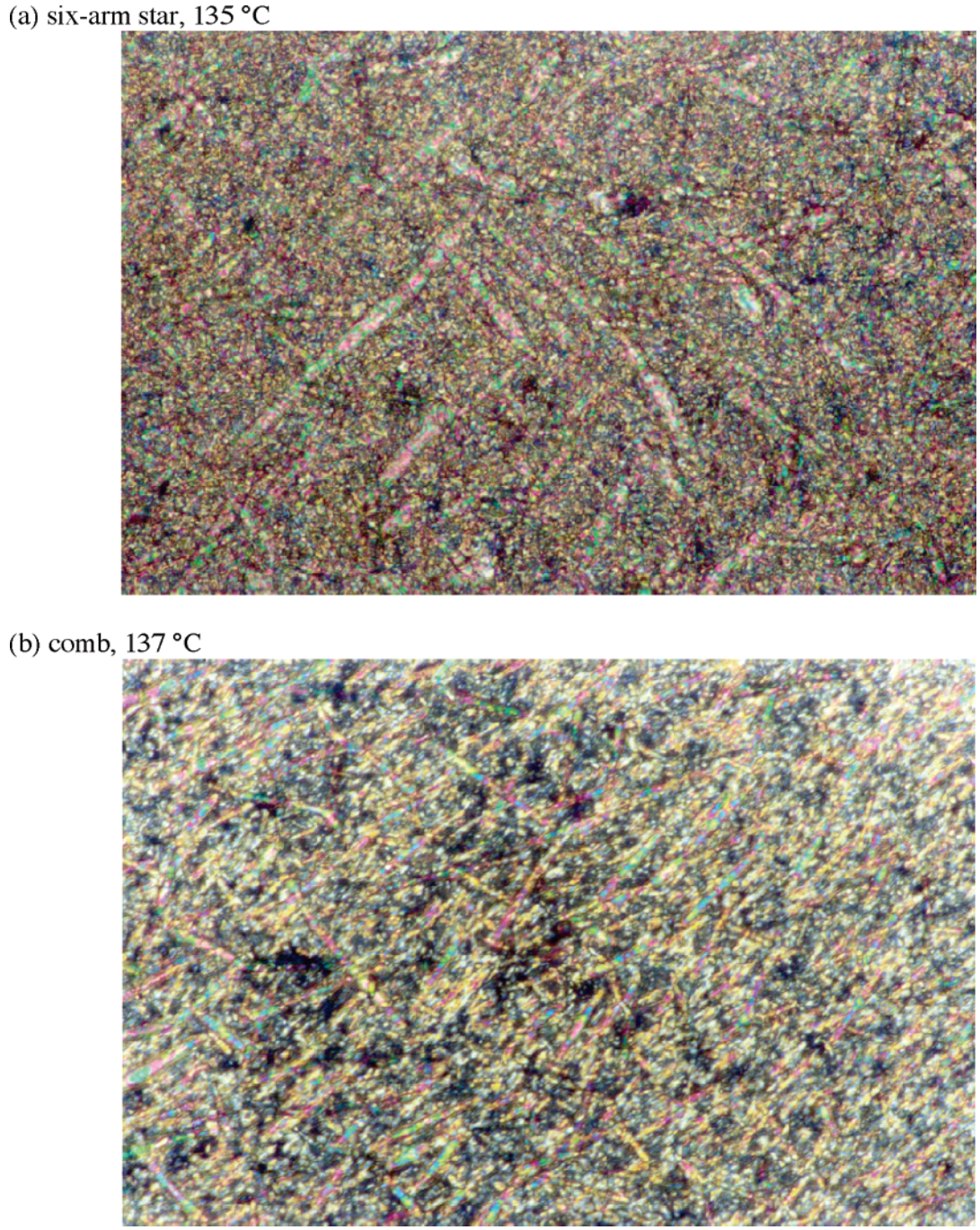

Figure 6. Polarized optical micrographs (200×) of the smectic A textures observed upon cooling six-arm star ($GPC_{PSt,THF}$ $DP_n = 68$, GPC_{LS} $DP_n = 353$) and comb[4] ($GPC_{PSt,THF}$ $DP_n = 128$, GPC_{LS}-equivalent $DP_n = 251$ based on equation from Table S1) poly[11-(4′-cyanophenyl-4″-phenoxy)-undecyl acrylate]s after annealing for 30 min at 3 °C below the isotropization temperatures.

polymer as a function of molecular weight in CH_2Cl_2. Comparison of the plateau values at $M_i = 10^6$, where the effect of the high core segment density is negligible, demonstrates that the contraction factors of the six-arm star ($g = 0.57$) and comb polymers with six branches ($g = 0.58$) are essentially equal. Although theories relating the contraction factor to the number of branches are based on the radii of gyration under theta conditions ($\nu = 0.50$),[19] which would therefore neglect the intramolecular mesogen-mesogen interactions present in these SCLCPs, g apparently varies little in a good vs a Θ solvent.[20] The value of $g = 0.57$ for the six-arm star polymers is higher than the values calculated for a conventional star polymer at the Gaussian limit with six monodisperse arms ($g = 0.44$) and six polydisperse arms ($g = 0.37$).[21] Assuming the theories are valid when $\nu = 0.36-0.39$, this indicates that the "six-arm star" polymers may have less than six arms; for example, the contraction factor should equal 0.52 for a star polymer with five monodisperse arms and 0.42 with five polydisperse arms. Nevertheless, the similarity of the contraction factors of the "six-arm star" polymers and comb polymers with six branches at $M_i = 10^6$ confirms the similarity of their structures at high molecular weight.

Thermotropic Behavior of the Six-Arm Star Polymers. Prior to fractionation to narrow their molecular weight distributions, the original six-arm star polymers were carefully purified to remove both residual copper complexes and unreacted monomer, since both can significantly affect the thermal behavior of poly[11-(4′-cyanophenyl-4″-phenoxy)undecyl acrylate].[6] Table 2 summarizes the thermotropic behavior of the purified and fractionated six-arm star polymers with $GPC_{PSt,THF}$-

Table 3. Infinite Molecular Weight Transition Temperatures of Poly[11-(4′-cyanophenyl-4″-phenoxy)undecyl acrylate]s Synthesized by Atom Transfer or Conventional Radical Polymerizations[a]

	transition temp (°C)					
	M_n from GPC_{PSt} in THF			M_n from GPC_{LS} in CH_2Cl_2		
architecture	g−s_C	s_C−s_A	s_A−i	g−s_C	s_C−s_A	s_A−i
linear (−$CH(CH_3)CO_2CH_3$/-Br endgroups)[6,9]	16	26	144	18	26	145
linear (−H/−Br end groups)[5,9]	16	25	147	14	23	144
three-arm star[6,9]	15	27	145	16	26	143
six-arm star	18	28	150	16	27	141
comb[4,9]	19	29	148	18	29	146
conventional radical and its fractions[6,9]	12	26	154		24	147

[a] M_n = number-average molecular weight, GPC_{PSt} = gel permeation chromatography relative to linear polystyrene; GPC_{LS} = GPC in CH_2Cl_2 using a three-angle (46, 90, and 134°) light scattering detector; g = glass, s_C = smectic C, s_A = smectic A, and i = isotropic.

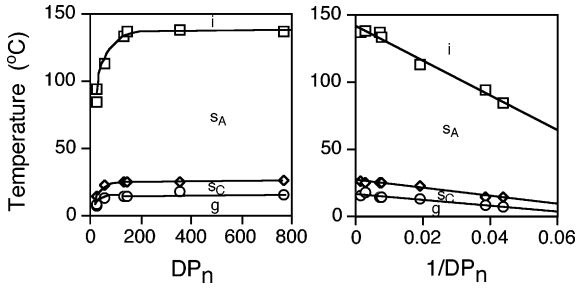

Figure 7. Dependence of the glass (g, ○), smectic C-smectic A (s_C−s_A, ◇), and smectic A-isotropic (s_A−i, □) phase transition temperatures of six-arm star poly[11-(4′-cyanophenyl-4″-phenoxy)undecyl acrylate]s as a function of the absolute number-average degree of polymerization and the inverse absolute number-average degree of polymerization determined by gel permeation chromatography in CH_2Cl_2 using a three-angle (46, 90, and 134°) light scattering detector. Infinite molecular weight transitions: g 16 s_C 27 s_A 141 i.

determined degrees of polymerization of 13−112 (PDI = 1.08−1.56). Figure 5 presents their normalized differential scanning calorimetry (DSC) traces on heating and on cooling. Upon heating, the polymers undergo a glass transition, which overlaps (except at very slow heating/cooling rates) a s_C−s_A transition, followed by isotropization from the s_A mesophase. As summarized in both Table 2 and Figure 5, all of the six-arm star polymers exhibit very narrow isotropization transitions (full width at half of the maximum peak intensity, fwhm = 3.27−9.02 °C), much like the comb polymers.[4] However, the breadth of the s_A−i transition increases slightly with decreasing molecular weight, evidently due to the limited miscibility of the core and/or end groups. The two polymers with the broadest polydispersities (PDI = 1.45−1.56) have the narrowest isotropization transitions (fwhm = 3.27−4.31 °C).

In contrast to the linear and three-arm star polymers,[6] which exhibit distinctive focal-conic fan textures immediately upon cooling from the isotropic melt into the s_A mesophase, the polarized optical micrograph shown in Figure 6a for the six-arm star polymer with GPC_{LS}-determined DP_n = 353 has a much finer s_A texture with a much larger number of defects after annealing for 30 min at 3 °C below the isotropization temperature. The focal-conic fan regions are barely detectable across the majority of the film, although some well-defined fans develop near the edges. Similarly, the polarized optical micrograph shown in Figure 6b of the highest molecular weight comb polymer synthesized previously[4] (GPC_{LS}-equivalent DP_n = 251) exhibits a fine texture with barely detectable focal-conic fan regions across the majority of the film after similar annealing, with more well-defined fans developing only near the edges. This demonstrates that the branching of both the six-arm star and comb polymers hinder their ability to rapidly order into larger liquid crystalline domains.

In contrast to the glass and s_A−s_C transitions, the large hexafunctional core also significantly depresses the isotropization temperature of the six-arm star polymers at the lowest degrees of polymerization compared to the transition temperatures of the linear[5,6] and three-arm star[6] polymers of similar chain lengths; the comb[4] polymers cannot be compared since they were not synthesized with correspondingly low degrees of polymerization. Figure 7 plots the transition temperatures of the six-arm star polymers as a function of both the GPC_{LS}-determined degrees of polymerization and inverse degrees of polymerization. Figure S1 in the Supporting Information plots the corresponding transition temperatures vs the $GPC_{PSt,THF}$-determined degrees of polymerization and inverse degrees of polymerization. The transition temperatures increase with increasing molecular weight and become independent of molecular weight after approximately 150 repeat units, which is slightly higher than that of the comb polymers,[4] or 35 polystyrene-equivalent repeat units. As summarized in Table 3, the isotropization temperature extrapolated to infinite absolute molecular weight ($DP_n^{-1} = 0$) is 141 °C, which is slightly lower than that of all of the other architectures. In contrast, the isotropization temperature extrapolated to infinite GPC_{PSt}-determined molecular weight is slightly higher than that of all of the other architectures, but most similar to that of the comb polymer. Nevertheless, the transition temperatures corresponding to infinite molecular weight do not differ significantly for the different architectures since the effect of end groups and branch points are minimized at high molecular weight.

Binary Blends of the Six-Arm Star Polymers. The long-held belief that the broad phase transitions often exhibited by SCLCPs prepared by nonliving polymerizations are due to polydispersity in molecular weight was supported by the narrower isotropization transitions of samples fractionated from poly[11-(4′-cyanophenyl-4″-phenoxy)undecyl acrylate] prepared by conventional radical polymerization compared to that of the original sample.[2] However, this implies that polymer chains within the same sample undergo phase transitions one chain length at a time, which is inconsistent with the narrow transitions shown in Figure 5 for all of the six-arm star polymers, including those with the broadest polydispersities. In addition, solid−liquid and liquid−liquid temperature vs composition diagrams demonstrate that the biphasic region of a mixture of compounds should only be broad or multimodal if the components of that mixture are not miscible in either or both phases that coexist at that transition.[22] This is exemplified by the DSC traces of the macroscopically phase separated ("unmixed") blends of two different six-arm star polymers shown in Figure 8, which were generated by computer summation of the DSC traces of the two individual components. Comparison to the intimately mixed blends of the corresponding polymers, also shown in Figure 8, therefore illustrates the miscibility or immiscibility of the two

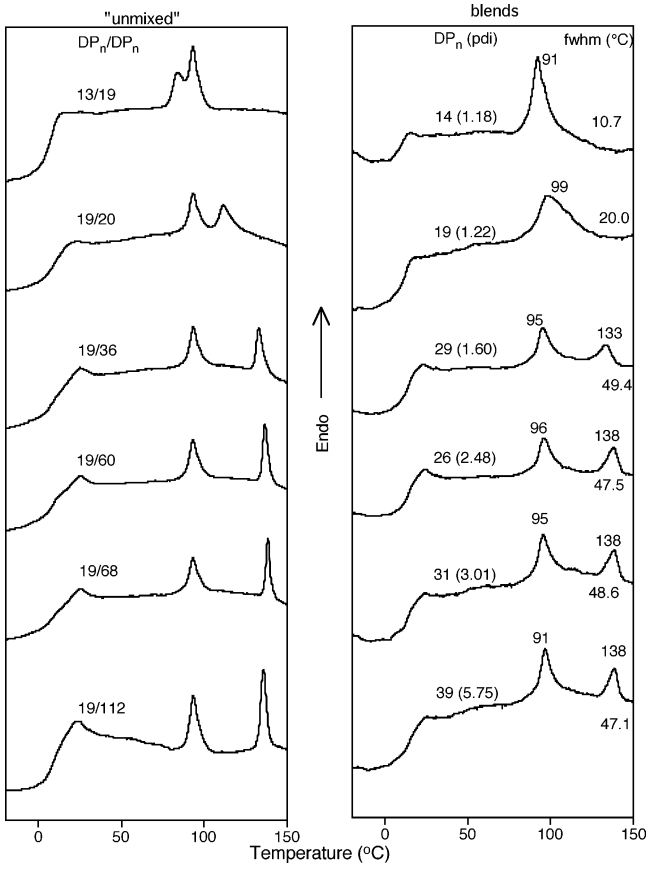

Figure 8. Normalized differential scanning calorimetry traces (10 °C/min) of 1:1 binary unmixed (physically separated) composites and blends of $DP_n = 19$ (PDI = 1.16) six-arm star poly[11-(4′-cyanophenyl-4″-phenoxy)undecyl acrylate] with the other six-arm star polymers ($GPC_{PSt,THF}$-determined $DP_n = 13-112$, PDI = 1.08−1.56).

components.

Figure 8 presents the DSC traces of unmixed and intimate blends of one of the lowest molecular weight six-arm polymer with one lower molecular weight and all of the higher molecular weight six-arm star polymers. Figure S2 in the Supporting Information presents the DSC traces of unmixed and intimate blends of the highest molecular weight six-arm star polymer with all of the lower molecular weight six-arm star polymers, and Figures S3−S5 present the corresponding DSC traces of the six-arm star polymers blended with linear, three-arm star, and comb polymers, respectively, to investigate the miscibility of the six-arm star poly[11-(4′-cyanophenyl-4″-phenoxy)undecyl acrylate]s with their topological isomers. Table 4 summarizes the average degree of polymerization, polydispersity and composition of these blends; most of the blends contain approximately equal amounts of the two components. The theoretical degrees of polymerization agree well with the measured degrees of polymerization only when the polydispersity of the sample is low.

Although the blends appear to be miscible when the two components have similar transition temperatures, the six-arm star polymers generally do not mix well with either the other six-arm star polymers or the other architectures; many of the samples are phase separated, with the two isotropization transition temperatures close to those of the pure components. Very few of the blends with different isotropization temperatures exhibit a monomodal endotherm at a temperature intermediate between the isotropization temperatures of the two components. The monomodal transitions are often broadened relative to those of the two components, which indicates that the two components have limited miscibility.

Table 4. Composition and Characterization of 1:1 Binary Blends of Poly[11-(4′-cyanophenyl-4″-phenoxy)undecyl acrylate]s Prepared by Atom Transfer Radical Polymerization

polymers **1**/**2**	composition (%)		theoretical	GPC_{PSt}[a]			fwhm[b]
DP_n/DP_n[a]	polymer **1**	polymer **2**	DP_n	DP_n	PDI	T_i (°C)	(°C)
Six-Arm Star/Six-Arm Star							
13/19	52	48	16	14	1.18	91	10.7
19/20	47	53	20	19	1.22	99	20.0
19/36	49	51	28	29	1.60	96, 133	49.4
19/60	49	51	40	26	2.48	96, 138	47.5
19/68	47	53	45	31	3.01	95, 138	48.6
19/112	51	49	61	39	5.75	97, 138	48.6
13/112	51	49	57	36	5.45	85, 135	60.2
20/112	49	51	67	70	3.78	136	30.2
36/112	50	50	73	115	2.20	136	7.06
60/112	51	49	86	159	1.91	141	2.75
68/112	51	49	90	183	1.79	138	3.53
Six-Arm Star/Linear[4,5]							
19/16	47	53	18	17	1.26	100, bimodal	35.3
19/18	48	52	18	14	1.18	100, bimodal	37.1
36/41	55	45	38	58	1.48	137	8.28
60/16	51	49	37	17	3.98	130	15.7
68/16	45	55	44	15	4.48	134	13.9
68/86	47	53	78	132	1.62	144	5.86
Six-Arm Star/Three-Arm Star[6,11]							
36/35	48	52	36	59	1.49	133	5.71
36/85	50	50	61	97	1.41	130	8.63
60/57	46	54	58	75	1.79	140	5.00
60/67	37	63	64	68	1.81	138	6.29
68/67	51	49	68	154	1.77	141	5.71
Six-Arm Star/Comb[4]							
60/87	48	52	72	92	2.10	140	4.00
68/87	50	50	76	108	1.70	140	3.20
112/127	24	76	122	125	1.54	142	5.00

[a] Number-average degree of polymerization (DP_n) and polydispersity (PDI = M_w/M_n) determined by gel permeation chromatography (GPC_{PSt}) in tetrahydrofuran at 35 °C relative to linear polystyrene using mean of UV and/or RI detectors. [b] Full width at half of the maximum peak intensity.

Figure 9 plots the breadth (fwhm) of the s_A-i transition as a function of the polydispersity of the binary blends of the six-arm star polymers, and includes similar data for the comb[4] polymer blends for comparison. This plot demonstrates that there is no correlation between the breadth of the transition and the polydispersity in molecular weight of the binary blends. For example, the fwhm of the binary blends involving the six-arm star and/or comb polymers with PDI = 1.4−1.7 range from 3 to 49 °C. We therefore consider the effect of the differences in the branching and end group densities of the two components, which vary for branched polymers of different molecular weight. Table S3 of the Supporting Information lists the branching and end group densities of the polymers used in the six-arm star blends, using both $GPC_{PSt,THF}$- and GPC_{LS}-determined molecular weights and normalized to chains of 50 repeat units. Table S4 lists the corresponding differences in branching and end group densities of the components of each six-arm star binary blend.

Figure 9 also plots the breadth of isotropization as a function of the differences in the branching and end group densities calculated based on the $GPC_{PSt,THF}$-determined molecular weights, and Figure 10 plots the breadth of isotropization as a function of the differences in the branching and end group densities calculated based on the GPC_{LS}-determined molecular weights. Although the fwhm values generally increase as the difference in branching density increases in both figures, the plots involving blends with linear polymers are not meaningful since the branching density of the linear polymers is zero, regardless of

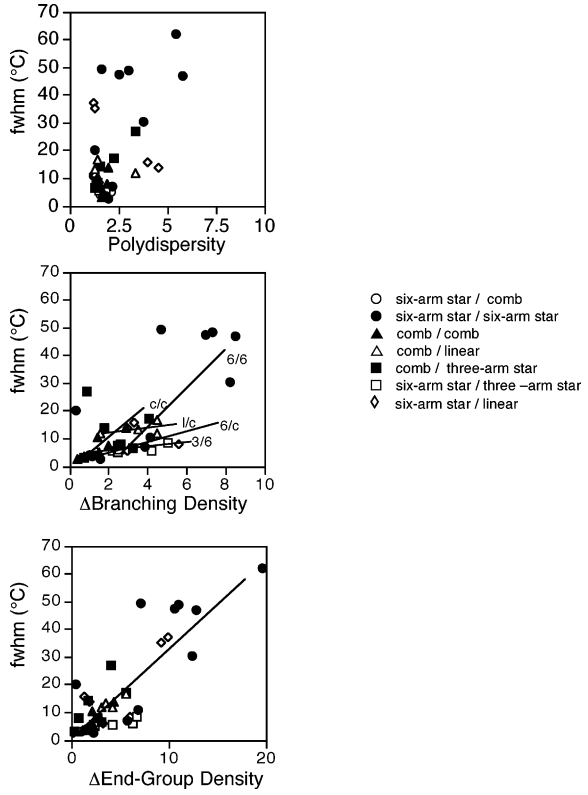

Figure 9. Dependence of the breadth of isotropization (fwhm = full width at half of the maximum peak intensity) of 1:1 binary blends of six-arm star and comb[4] poly[11-(4′-cyanophenyl-4″-phenoxy)undecyl acrylate]s with various architectures as a function of the blends' polydispersity (PDI = M_w/M_n) in molecular weight, difference in branching density (normalized to chains of 50 repeat units), and difference in end group density (normalized to chains of 50 repeat units) using molecular weight data measured by gel permeation chromatography in tetrahydrofuran relative to linear polystyrene.

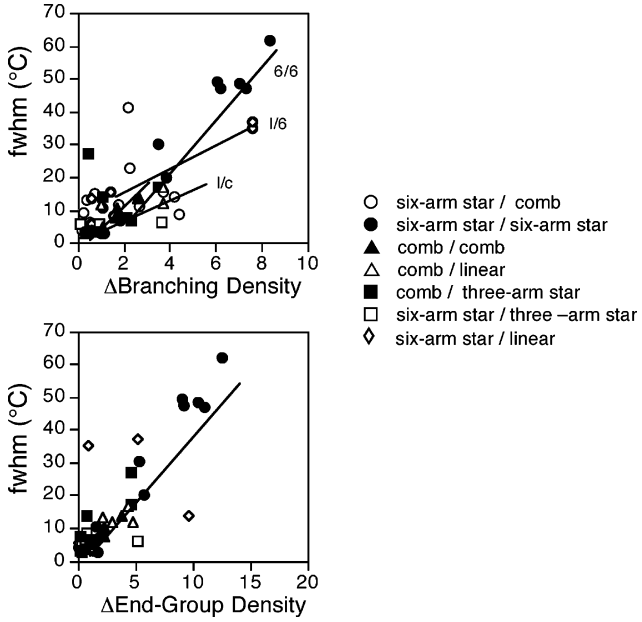

Figure 10. Dependence of the breadth of isotropization (fwhm = full width at half of the maximum peak intensity) of 1:1 binary blends of six-arm star and comb[4] poly[11-(4′-cyanophenyl-4″-phenoxy)undecyl acrylate]s with various architectures as a function of the blends' difference in branching density and difference in end group density (both normalized to chains of 50 repeat units) using molecular weight data measured by gel permeation chromatography in CH_2Cl_2 using a three-angle light scattering detector.

molecular weight. (The difference in branching density of linear/linear blends is therefore also always zero.) The difference in end group density is more meaningful since the end group density of polymers of any topology is a nonzero value. Although the data are somewhat scattered, the breadth of the s_A-i phase transition of binary blends of six-arm star and/or comb poly[11-(4′-cyanophenyl-4″-phenoxy)undecyl acrylate]s increases roughly linearly with the difference in end group density (normalized to 50 repeat units) of the two components.

Conclusions

The solution and thermotropic behavior of the six-arm star poly[11-(4′-cyanophenyl-4″-phenoxy)undecyl acrylate]s are similar to those of the comb poly[11-(4′-cyanophenyl-4″-phenoxy)-undecyl acrylate]s with six branches. Like the comb polymers, there is no evidence for aggregation of the six-arm star polymers in CH_2Cl_2. Although the six-arm star and comb polymers elute differently in gel permeation chromatography, their radii of gyration are similar, and both polymers have a spherical shape in CH_2Cl_2. The similarity of their structures is also confirmed by the similarity of their contraction factors at $M_i = 10^6$, although the value of the contraction factor ($g = 0.57$) of the "six-arm star" polymers indicates that they may have less than six arms. Both the six-arm star and comb polymers exhibit very narrow smectic A−isotropic transitions in the solid state, although the large hexafunctional core significantly depresses the isotropization temperature at low molecular weights. The six branches of both the six-arm star and comb polymers hinder their ability to rapidly order into larger liquid crystalline domains, and the polarized optical microscope textures of their smectic A mesophases therefore have many defects and are indistinctive. The transition temperatures of the six-arm star polymers become independent of molecular weight after approximately 150 repeat units, which is slightly higher than that of the comb polymers. The six-arm star polymers generally do not mix well with either the other six-arm star polymers or the other architectures, and the breadth of the s_A-i phase transition of binary blends involving the six-arm star and/or comb polymers increases roughly linearly with the difference in end group density (normalized to 50 repeat units) of the two components.

Acknowledgment is made to the National Science Foundation for support of this research through DMR-0322338. We also acknowledge Ms. Chun Chang and Mr. Steven R. Grunwald for synthesizing the comb and some of the linear and three-arm star polymers used in the polymer blends.

Supporting Information Available: Tables of linear equations corresponding to the data in Figure 1, composition of the blends used for conformation anlysis, values of the branching and end group densities, and differences in the branching and end group densities of the polymers used in the binary blends and figures showing the dependence of the transition temperatures on GPC_{PSt}-determined DP_n and DP_n^{-1} and DSC scans of binary blends of six-arm star polymers with six-arm star, linear, three-arm star, and comb polymers. This material is available free of charge via the Internet at http://pubs.acs.org.

References and Notes

(1) (a) Pugh, C.; Kiste, A. L. *Prog. Polym. Sci.* **1997**, *22*, 601−691. (b) Pugh, C.; Kiste, A. L. In *Handbook of Liquid Crystals*; Demus, D., Goodby, J. W., Gray, G. W., Spiess, H. W., Vill, V., Eds.; VCH: Weinheim, Germany, 1998; Vol. 3, Chapter 3.
(2) Kostromin, S. G.; Talroze, R. V.; Shibaev, V. P.; Plate, N. A. *Makromol. Chem., Rapid Commun.* **1982**, *3*, 803−808.

(3) Pugh, C.; Fan, G.; Kasko, A. M. *Macromolecules* **2005**, *38*, 8071−8077.
(4) Chang, C.; Pugh, C. *Macromolecules* **2001**, *34*, 2027−2039.
(5) Kasko, A. M.; Grunwald, S. R.; Pugh, C. *Macromolecules* **2002**, *35*, 5466−5474.
(6) Kasko, A. M.; Heintz, A. M.; Pugh, C. *Macromolecules* **1998**, *31*, 256−271.
(7) (a) Wang, J.-S.; Matyjaszewski, K. *Macromolecules* **1995**, *28*, 7572−7573. (b) Patten, T. E.; Xia, J.; Abernathy, T.; Matyjaszewski, K. *Science* **1996**, *272*, 866−868.
(8) g = glass; s_C = smectic, C.
(9) Kasko, A. M.; Pugh, C. *Macromolecules* **2004**, *37*, 4993−5001.
(10) According to ^{1}H NMR analysis, the macroinitiator used to synthesize the copolymers contained 87 mol % mesogenic repeat units and 13 mol % repeat units containing the initiating site, which corresponds to 31 mesogenic repeat units and five initiating sites dispersed along the backbone (plus one initiating site at the terminus) of a macroinitiator with $M_n = 1.44 \times 10^4$. Following grafting, the total $DP_n = [M_{n,comb} - 167.01 - (5)(251.08)]/419.56$, in which 167.01 is the molecular weight in g/mol of the end groups of the polymer backbone, 251.08 is the molecular weight in g/mol of the initiating repeat units plus the bromine end group of the grafts, and 419.56 is the molecular weight in g/mol of the mesogenic repeat units. Thus, DP_n of each of the six grafts is $DP_{n,graft} = (DP_{n,total} - 31)/6$.
(11) (a) Kasko, A. M.; Grunwald, S. R.; Pugh, C. Manuscript in preparation. (b) Grunwald, S. R.; M.S. Thesis, University of Akron, 2004.
(12) (a) Sigwalt, P. *Makromol. Chem.*−*Macromol. Symp.* **1991**, *47*, 179−201. (b) Matyjaszewski, K. *J. Polym. Sci., Polym. Chem. Ed.* **1993**, *31*, 995−999. (c) Matyjaszewski, K. *Macromolecules* **1993,** *26*, 1787−1788.
(13) GPC_{LS} measures the absolute weight-average molecular weight at each elution slice, in which each elution slice of the GPC chromatogram corresponds to a single size polymer ($M_n = M_w$) or a fraction of very narrow polydispersity. Therefore, each moment (M_n, M_w, M_z, etc.) of the molecular weight distribution can be considered an absolute molecular weight.
(14) (a) Jackson, C.; Chen, Y. J.; Mays, J. W. *J. Appl. Polym. Sci.* **1996**, *59*, 179−188. (b) Temyanko, E.; Russo, P. S.; Ricks, H. *Macromolecules* **2001**, *34*, 582−586.
(15) Wyatt, P. J. *Anal. Chim. Acta* **1993**, *272*, 1−40.
(16) Burchard, W. *Adv. Polym. Sci.* **1999**, *143*, 113−194.
(17) (a) Khasat, N.; Pennisi, R. W.; Hadjichristidis, N.; Fetters, L. J. *Macromolecules* **1988**, *21*, 1100−1106. (b) Roovers, J.; Toporowski, P.; Martin, J. *Macromolecules* **1989**, *22*, 1897−1903. (c) Roovers, J.; Zhou, L. L.; Toporowski, P. M.; van der Zwan, M.; Iatrou, H.; Hadjichristidis, N. *Macromolecules* **1993**, *26*, 4324−4331. (d) Baek, K. Y.; Kamigaito, M.; Sawamoto, M. *J. Polym. Sci., Polym. Chem. Ed.* **2002**, *40*, 2245−2255.
(18) Flory, P. J. *Principles of Polymer Chemistry*; Cornell University Press: Ithaca, NY, 1953.
(19) Zimm, B. H.; Stockmayer, W. H. *J. Chem. Phys.* **1949**, *17*, 1301−1314.
(20) Douglas, J. F.; Roovers, J.; Freed, K. F. *Macromolecules* **1990**, *23*, 4168−4180 and references therein.
(21) For star polymers with f Gaussian arms, $g = (3f - 2)/f^2$ if the arm lengths are monodisperse,[19] and $g = 3f/(f + 1)^2$ if the arm lengths are polydisperse.[16]
(22) See, for example: Vemulapalli, G. K. *Physical Chemistry*, 3rd ed.; Prentice Hall: Englewood Cliffs, NJ, 1993; Chapter 9.3.

MA060807X